

High-Field Hall Resistivity and Magnetoresistance of Electron-Doped $\text{Pr}_{2-x}\text{Ce}_x\text{CuO}_{4-\delta}$

Pengcheng Li,¹ F. F. Balakirev,² and R. L. Greene¹

¹*Center for Superconductivity Research and Department of Physics, University of Maryland, College Park, Maryland 20742-4111, USA*

²*NHMFL, Los Alamos National Laboratory, Los Alamos, New Mexico 87545, USA*

(Received 4 December 2006; published 25 July 2007)

We report resistivity and Hall effect measurements in electron-doped $\text{Pr}_{2-x}\text{Ce}_x\text{CuO}_{4-\delta}$ films in magnetic field up to 58 T. In contrast to hole-doped cuprates, we find a surprising nonlinear magnetic field dependence of Hall resistivity at high field in the optimally doped and overdoped films. We also observe a crossover from quadratic to linear field dependence of the positive magnetoresistance in the overdoped films. A spin density wave induced Fermi surface reconstruction model can be used to qualitatively explain both the Hall effect and magnetoresistance.

DOI: [10.1103/PhysRevLett.99.047003](https://doi.org/10.1103/PhysRevLett.99.047003)

PACS numbers: 74.25.Fy, 71.10.Hf, 73.43.Nq, 74.72.-h

Electron-doped (*n*-doped) cuprate superconductors have exhibited enough similarities with their hole-doped (*p*-doped) high- T_c counterparts so that any eventual rationalization of the phenomenon of high temperature superconductivity (SC) would have to treat both poles of the doping spectrum in the similar manner. Some of the key phenomena realized in both types of high- T_c compounds, such as the competition between antiferromagnetism (AFM) and SC or the anomalous temperature dependence of the transport coefficients, pose challenging questions for the condensed matter physics. Meanwhile, a number of studies in the past years have identified distinct differences in the properties of *n*-doped and *p*-doped cuprates. Understanding the causes of the differences and similarities may lead to understanding of the phenomenon of high temperature superconductivity. Among the distinctive properties, angle resolved photoemission spectroscopy (ARPES) experiments [1–3] in *n*-doped cuprates have revealed a small electronlike Fermi surface (FS) pocket at $(\pi, 0)$ in the underdoped region, and a simultaneous presence of both electron- and holelike pockets near optimal doping. This clarifies the long-standing puzzle that transport in these materials exhibits unambiguous *n*-type carrier behavior at low-doping and two-carrier behavior near optimal doping [4–7]. Recent low temperature normal state Hall effect measurements [8] on $\text{Pr}_{2-x}\text{Ce}_x\text{CuO}_{4-\delta}$ (PCCO) show a sharp kink of the Hall coefficient at a critical doping $x = 0.16$, which suggests a quantum phase transition (QPT) at this doping. Early μSR measurements found that the AFM phase starts at $x = 0$ and persists up to, or into, the SC dome [9]. Neutron scattering experiments [10] show an AFM phase above critical field in an optimally doped *n*-type cuprates, but no such phase on the overdoped side. Optical conductivity experiments [11] reveal a partial normal state gap opening at a certain temperature in the underdoped region, but no such gap is found above the critical doping. A spin density wave (SDW) model [12,13] was proposed, which gives a plausible, but qualitative,

explanation to these observations. In this model, SDW ordering would induce a Fermi surface (FS) reconstruction and result in an evolution from an electron pocket to the coexistence of electron- and holelike pockets with increasing doping, and eventually into a single holelike FS. The SDW gap amplitude decreases from the underdoped side and vanishes at the critical doping.

Recently, an inelastic neutron scattering measurement on $\text{Nd}_{2-x}\text{Ce}_x\text{CuO}_{4-\delta}$ (NCCO) by Motoyama *et al.* [14] found that long range ordered AFM vanishes near the SC dome boundary, $x = 0.13$. They claim that SC and AFM do not coexist and that the QPT occurs at $x = 0.13$, which differs from the results mentioned above. Therefore, the presence of a QPT and the location of the quantum critical point (QCP) in *n*-doped cuprates is still under considerable debate. Whether the QCP is under the SC dome and whether the SC and AFM coexist are important issues to clarify. Similar issues exist for the *p*-doped cuprates, although the nature of any order parameter (in the pseudogap phase) which might disappear at a QCP under the SC dome is unknown.

In this Letter, for the first time, we used a high magnetic field to investigate the transport behavior in *n*-doped PCCO over a wide range of doping and temperature. We performed Hall resistivity and *ab*-plane resistivity measurements on PCCO films from underdoped (UND) ($x = 0.11$) to overdoped (OVD) ($x = 0.19$) for temperature down to $T = 1.5$ K and magnetic field up to 58 T. We find that both the Hall resistivity and magnetoresistance (MR) show a dramatic change near optimally doped (OPD) $x = 0.15$. A surprising nonlinear Hall resistivity for $x \geq 0.15$ is observed, while linearity of the Hall resistivity persists up to 58 T in the UND films. In the OVD region, a crossover of MR from a low field quadratic behavior to a high-field linear dependence is found, which is in agreement with a recent theory on the magnetotransport properties near a metallic QCP [15]. Our results suggest that the QPT occurs around optimal doping in the *n*-doped cuprates.

PCCO c -axis oriented films with various Ce concentrations ($x = 0.11$ to 0.19) were fabricated by pulsed laser deposition on (100) oriented SrTiO₃ substrates [16]. Since the oxygen content has an influence on both the SC and normal state properties of the material [5], we optimized the annealing process for each Ce concentration as in Ref. [8]. The sharp transition, low residual resistivity, and the Hall coefficient are exactly the same as in our previous report [8]. We note that the exact content of oxygen cannot be determined in films, and we use the T_c values of the annealed films and Ce content to determine the temperature versus doping phase diagram. Photolithography and ion mill techniques are used to pattern the films into a standard six-probe Hall bar. Resistivity and Hall effect measurements were carried out in a 60 T pulsed magnetic field at the NHMFL. The magnetic field is aligned perpendicular to the ab -plane of the films. Possible eddy current heating was carefully considered and reduced.

The Hall effect is measured for all the doped PCCO films. At low field for H up to 14 T, the Hall resistivity $\rho_{xy}(H)$ is linear at all dopings and temperatures [8], and the Hall coefficient R_H is determined as ρ_{xy}/H . Figure 1(a) shows the temperature dependence of R_H measured at 14 T for all the PCCO films, similar to our previous report [8]. In high fields, we find that the linear negative $\rho_{xy}(H)$ (electronlike) persists up to 58 T in the UND films at temperatures below 100 K (the limit of our present data). Figure 1(b) shows the $\rho_{xy}(H)$ data for an UND $x = 0.13$ film ($T_c = 11$ K). For the nonsuperconducting $x = 0.11$, a similar behavior is observed (not shown). In contrast, as x approaches the OPD $x = 0.15$, $\rho_{xy}(H)$ behaves differently. As shown in Fig. 2(a), at low temperatures ($T < 50$ K) $\rho_{xy}(H)$ is negative and linear up to about 30 T but then starts curving towards positive slopes. This nonlinearity begins at higher fields as the temperature is increased, and it appears that $\rho_{xy}(H)$ will become linear above 50 K, but we were not able to obtain data above 50 K on this film. For the OVD film $x = 0.16$, the low temperature $\rho_{xy}(H)$ is positive and slightly nonlinear at high field. The nonlinearity becomes more prominent near the temperature where

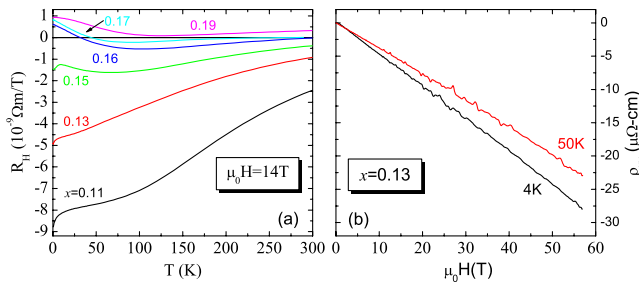


FIG. 1 (color online). (a) Normal state Hall coefficient R_H versus temperature for PCCO films measured at $\mu_0 H = 14$ T ($H \perp ab$ and $H > H_{c2}$). (b) Hall resistivity ρ_{xy} versus H for the UND PCCO $x = 0.13$ film at $T = 4$ K and 50 K.

R_H changes sign (about 25 K), but then a negative linearity of $\rho_{xy}(H)$ is found at higher temperatures. The positive slope of $\rho_{xy}(H)$ at high field for $T \leq 75$ K indicates a holelike contribution. A similar behavior was observed for the $x = 0.17$ film as shown in Fig. 2(c). For a highly OVD film, $x = 0.19$, in which R_H is always positive, but with a minimum around 120 K [see Fig. 1(a)], a strong field dependence of $\rho_{xy}(H)$ is observed above 30 K, while $\rho_{xy}(H)$ is linear at low temperatures. We note that this nonlinear $\rho_{xy}(H)$ in the OPD and OVD films is in striking contrast to the linear $\rho_{xy}(H)$ found up to 60 T in p -doped Bi₂Sr_{2-x}La_xO_{6+δ} at all dopings and temperatures [17].

The in-plane magnetoresistance (MR) is also measured in PCCO films, and we find that the high-field MR varies greatly with doping as well. In the UND region, a large low temperature negative MR (nMR) is observed, similar to the prior work [18]. For $x = 0.11$ ($T < 100$ K), this nMR persists up to 58 T, while for $x = 0.13$ ($T < 30$ K), the nMR tends to saturate at high field, as shown in the inset of Fig. 3(a). A positive MR is recovered for $T > 50$ K, and it follows a quadratic field (H^2) dependence. For the OPD $x = 0.15$, the low temperature nMR reverses to a positive MR at $H \sim 30$ T [Fig. 3(b)]. For $T > 20$ K, this positive MR also obeys H^2 . In the OVD films, a positive MR is found in the normal state, but the field dependence of the MR is surprisingly different as the temperature is increased. Figures 3(c) and 3(d) show the MR along with the first field derivative of MR ($d\rho_{xx}(H)/dH$) for $x = 0.17$. At low temperatures ($T < 20$ K), a nearly linear MR for $H > H_{c2}$ is found, as seen from the roughly constant behavior of the $d\rho_{xx}(H)/dH$ plot. However, in the intermediate temperature range where the nonlinear $\rho_{xy}(H)$ is prominent, we find that $d\rho_{xx}(H)/dH$ increases monotonically at lower field and then saturates to a nearly constant

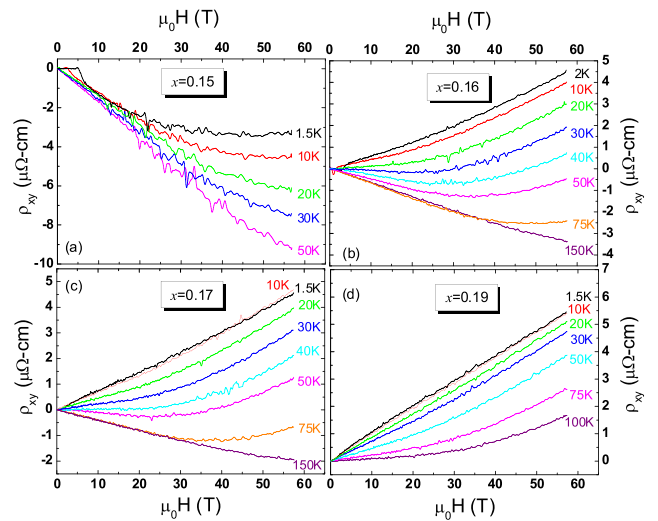


FIG. 2 (color online). Hall resistivity ρ_{xy} versus H for the OPD and OVD PCCO films (a) $x = 0.15$, (b) $x = 0.16$, (c) $x = 0.17$, (d) $x = 0.19$.

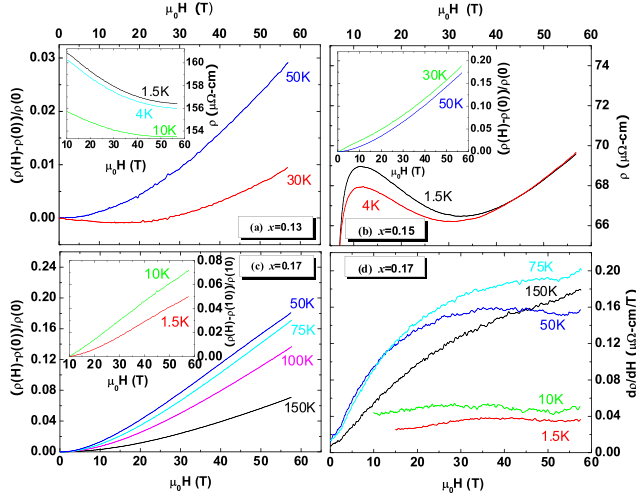


FIG. 3 (color online). In-plane resistivity versus H ($H \perp ab$) for PCCO films (a) $x = 0.13$, (b) 0.15 , (c) 0.17 , and (d) first derivative plots for 0.17 . Insets show the magnetoresistance in a different temperature range from the main panels.

value at higher field. The low field linear increase of $d\rho_{xx}(H)/dH$ indicates a quadratic MR and the high-field saturation indicates a linear MR. A similar linear MR is also observed in the $x = 0.16$ and 0.19 films at low temperatures where the linear $\rho_{xy}(H)$ is in present. At higher temperatures, the MR changes from quadratic at low field to linear at high field.

The nonlinear behavior of $\rho_{xy}(H)$ displayed on Fig. 2 can be simulated within the framework of a conventional two-band Drude model. The Drude model assumes field-independent carrier density and relaxation time, in which case $\rho(H)$ can be written as [19]:
$$\rho_{xy}(H) = \frac{\sigma_h^2 R_h - \sigma_e^2 R_e - \sigma_h^2 \sigma_e^2 R_h R_e (R_h - R_e) H^2}{(\sigma_e + \sigma_h)^2 + \sigma_e^2 \sigma_h^2 (R_h - R_e)^2 H^2} H$$
 and
$$\rho_{xx}(H) = \frac{(\sigma_h + \sigma_e) + \sigma_h \sigma_e (\sigma_h R_h^2 + \sigma_e R_e^2) H^2}{(\sigma_h + \sigma_e)^2 + \sigma_h^2 \sigma_e^2 (R_h - R_e)^2 H^2} [\sigma_e(h) \text{ and } R_e(h) \text{ are electrical conductivity and Hall coefficient of the electron (hole) band}].$$
 Using the relation of $\sigma_0 = \sigma_h + \sigma_e$ (σ_0 is the zero field normal state conductivity), one parameter is eliminated. We attempted to fit our $\rho_{xy}(H)$ and MR data, but we could not fit both $\rho_{xy}(H)$ and $\rho_{xx}(H)$ with the same fitting parameters for any of the films. We also find that the parameters by fitting $\rho_{xy}(H)$ alone are in conflict with ARPES results. The hole and electron densities at $T = 10$ K for $x = 0.15$ from fitting $\rho_{xy}(H)$ are $n_h = \frac{1}{R_h |e|} = 6.0 \times 10^{20}/\text{cm}^3$ and $n_e = 3.5 \times 10^{20}/\text{cm}^3$, which disagree with $n_h = 3.6 \times 10^{20}/\text{cm}^3$ and $n_e = 1.8 \times 10^{21}/\text{cm}^3$, the estimate from the areas of the hole and electron pockets in ARPES [1,20]. The departure of our fits from the experimental data is most likely due to the simple assumption of a field-independent charge density and scattering in the Drude model. This is unlikely to be valid for the n -doped cuprates with their complex FS. It is likely that there is a strong anisotropic scattering, as found in p -doped cuprates

[21]. Therefore, the simple Drude model is not sufficient to explain the high-field magnetotransport in PCCO. A modified model with consideration of field dependent charge density or scattering might explain our data; however, this is beyond our present knowledge and the scope of this Letter.

We now discuss a qualitative (and speculative) explanation for our data. As seen from the phase diagram of n -doped cuprates (see Fig. 4), the long range ordered AFM phase persists up to a critical doping of x_c (exact location is under debate). In the UND region, a large SDW gap (Δ_{SDW}) opens at certain temperatures [11]. In a magnetic field comparable to the gap (i.e., $\mu_B B \sim \Delta_{\text{SDW}}$), one expects a suppression of Δ_{SDW} by the field and a consequent change of the FS. Since $\rho_{xy}(H)$ is sensitive to the shape of the FS, a nonlinear ρ_{xy} in high field might emerge. Applying this picture to our data, let us start from the lowest temperature (1.5 K). In the UND $x = 0.11$ and 0.13 , we find that the linear $\rho_{xy}(H)$ persists up to 58 T [Fig. 1(b)], suggesting that the field is not sufficient to destroy the large SDW gap. Therefore, the electronlike pocket still survives to high field for all the temperatures measured. As the doping approaches the critical doping, Δ_{SDW} decreases rapidly. When the magnetic field is strong enough to suppress the smaller gap, the holelike pocket emerges and will contribute to $\rho_{xy}(H)$. The positive slope of $\rho_{xy}(H)$ at high field in the OPD film $x = 0.15$ suggests the suppression of the SDW gap and a contribution from the hole band.

In the OVD region for $x \geq 0.16$, the linear positive $\rho_{xy}(H)$ at the lowest temperature strongly suggests the absence of the SDW gap and a holelike behavior. The nonlinearity of $\rho_{xy}(H)$ appears at higher temperatures for

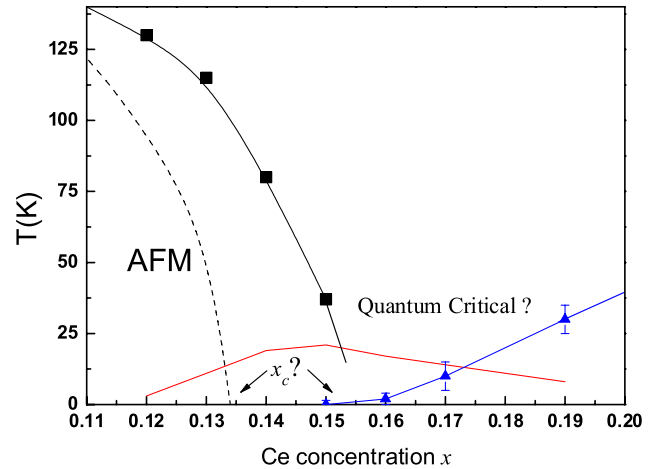


FIG. 4 (color online). A phase diagram for n -doped cuprates. Black squares and dashed line are the controversial AFM transition temperature from Ref. [9,10,14] respectively. The solid line is T_c . The triangles mark the temperature above which the nonlinear $\rho_{xy}(H)$ appears for each doping.

larger x , as seen in Fig. 2. Notice that a slightly nonlinear $\rho_{xy}(H)$ is found for $x = 0.16$ even at the lowest temperature 2 K, while in $x = 0.17$ and 0.19 , this nonlinearity starts to appear at temperatures above 10 K and 30 K, respectively, as indicated with blue triangles in Fig. 4.

The observed nonlinearity in $\rho_{xy}(H)$ in the OVD region in the intermediate temperature range suggests a competition between electron and hole bands. This unusual nonlinearity of $\rho_{xy}(H)$ might arise from spin fluctuations of SDW order in a quantum critical region associated with the QPT at x_c . As shown in Fig. 4, thermally activated spin fluctuations (gaplike) in the OVD region at finite temperature could result in a mix of electron and hole contributions to $\rho_{xy}(H)$. This could be responsible for the sign change of the $R_H(T)$ [Fig. 1(a)] and the positive upturn of the $\rho_{xy}(H)$ at high fields. In the critical region, an external perturbation, such as temperature or magnetic field, could change the relative impact of the two bands. The onset temperature of the high-field nonlinear $\rho_{xy}(H)$ shifts towards a higher temperature as x increases, which strongly suggests the system is further away from the critical region at higher doping.

Interestingly, we notice that our MR is also qualitatively consistent with the SDW model. In the UND region, the low temperature nMR persists and saturates in high field, suggesting that the nMR is related to spin scattering [18]. At optimal doping, a positive MR is recovered at a field where $\rho_{xy}(H)$ changes slope. The complete suppression of the nMR suggests the reduction of the spin contribution. For the OVD films ($x \geq 0.16$), we find that the crossover in the field dependence of the MR is consistent with a recent theory. It has been shown [15] that near a metallic QCP, a quadratic MR ($\frac{\Delta\rho}{\rho} \sim H^2$) is expected for a system with a SDW gap and a linear MR without a gap. As shown in Fig. 3(c) and 3(d), in the intermediate temperature range, the MR changes from quadratic to linear as the field increases while it is always linear at low temperature. This suggests the absence of the SDW gap at low temperature. In the spin fluctuation region, the field suppressed spin contribution could be responsible for the recovery of the linear MR at high field. At much higher temperatures (above 150 K), the quadratic MR is restored.

We have shown that our $\rho_{xy}(H)$ and $\rho_{xx}(H)$ are qualitatively consistent with the SDW model, suggesting that the QPT occurs near or just above the optimal doping. However, the SDW gap closing field (about 30–40 T for $x = 0.15$) obtained from the nonlinear $\rho_{xy}(H)$ is much smaller than that from the optics measurements [11]. Further quantitative theoretical calculations are needed to

resolve this issue and to explain in detail the $\rho_{xy}(T, H)$ and $\rho_{xx}(T, H)$ results that we report here.

In summary, we performed high-field resistivity and Hall effect measurements in the n -doped cuprate $\text{Pr}_{2-x}\text{Ce}_x\text{CuO}_{4-\delta}$. We find an anomalous nonlinear Hall resistivity at high field above optimal doping at certain temperatures. We also observed a crossover of the field dependence of magnetoresistance at high field in the overdoped region. Our results are qualitatively consistent with the spin density wave gap induced Fermi surface rearrangement model [12], and also support the view that a quantum phase transition occurs under the superconducting dome in this material.

We are grateful to the fruitful discussions with A. Millis, V. Yakovenko, and A. Chubukov. P.L. and R.L.G. acknowledge the support of NSF Grant No. DMR-0352735. The work at NHMFL was supported by NSF and DOE.

-
- [1] N. P. Armitage *et al.*, Phys. Rev. Lett. **88**, 257001 (2002).
 - [2] H. Matsui *et al.*, Phys. Rev. Lett. **94**, 047005 (2005).
 - [3] H. Matsui *et al.*, Phys. Rev. Lett. **95**, 017003 (2005).
 - [4] Z. Z. Wang *et al.*, Phys. Rev. B **43**, 3020 (1991).
 - [5] W. Jiang *et al.*, Phys. Rev. Lett. **73**, 1291 (1994).
 - [6] P. Fournier *et al.*, Phys. Rev. B **56**, 14149 (1997).
 - [7] F. Gollnik and M. Naito, Phys. Rev. B **58**, 11734 (1998).
 - [8] Y. Dagan *et al.*, Phys. Rev. Lett. **92**, 167001 (2004).
 - [9] G. M. Luke *et al.*, Phys. Rev. B **42**, 7981 (1990); T. Uefuji *et al.*, Physica C (Amsterdam) **378**, 273 (2002).
 - [10] H. Kang *et al.*, Nature (London) **423**, 522 (2003); M. Fujita *et al.*, Phys. Rev. Lett. **93**, 147003 (2004).
 - [11] A. Zimmers *et al.*, Europhys. Lett. **70**, 225 (2005); Y. Onose *et al.*, Phys. Rev. Lett. **87**, 217001 (2001).
 - [12] J. Lin and A. J. Millis, Phys. Rev. B **72**, 214506 (2005).
 - [13] A. J. Millis *et al.*, Phys. Rev. B **72**, 224517 (2005).
 - [14] E. M. Motoyama *et al.*, Nature (London) **445**, 186 (2007).
 - [15] J. Fenton and A. J. Schofield, Phys. Rev. Lett. **95**, 247201 (2005).
 - [16] E. Maiser *et al.*, Physica (Amsterdam) **297C**, 15 (1998); J. L. Peng *et al.*, Phys. Rev. B **55**, R6145 (1997).
 - [17] F. Balakirev *et al.*, Nature (London) **424**, 912 (2003).
 - [18] Y. Dagan *et al.*, Phys. Rev. Lett. **94**, 057005 (2005).
 - [19] N. W. Ashcroft and N. D. Mermin, *Solid State Physics* (Saunders College Publishing, Philadelphia, 1976), p. 240.
 - [20] The electron and hole densities are obtained from the size of the electron and hole FS pockets, i.e., $n = A/2\pi^2$ (A is the area of the electron(hole) pocket from the ARPES in Ref. [1] and a SDW model calculation [12,13]), with G. Blumberg and M. Qazilbash (private communication).
 - [21] M. Abdel-Jawad *et al.*, Nature Phys. **2**, 821 (2006).